Available online at www.sciencedirect.com
ScienceDirect
Journal of the European Ceramic Society 30 (2010) 2173–2181
www.elsevier.com/locate/jeurceramsoc

Mechanical properties of ZrB_2–SiC($ZrSi_2$) ceramics

Oleg N. Grigoriev *, Boris A. Galanov, Valerii A. Kotenko, Sergey M. Ivanov, Alexandr V. Koroteev, Nikolay P. Brodnikovsky

Institute for Problems in Materials Science NAS, Kiev, Ukraine

Available online 16 May 2010

Abstract

Mechanical properties of ZrB_2–SiC and ZrB_2–$ZrSi_2$–SiC ceramics in the temperature range from 20 to 1400 °C were studied. It was found that the introduction of zirconium silicide resulted in pore-free ceramics having bending strengths of 400–500 MPa over a wide range of boride–carbide compositions. Zirconium silicide additive did not lead to significant strength and hardness changes at low temperature, but essentially increased Weibull modulus, and, therefore, the reliability of the ceramics. However, zirconium silicide additions resulted in noticeably reduced bending strength in ZrB_2–SiC based composites at 1400 °C.

Keywords: Composites; Borides; Fracture; Hardness; Strength

1. Introduction

Ceramic borides, such as hafnium diboride (HfB_2) and zirconium diboride (ZrB_2), are materials which have been referred to as Ultra High Temperature Ceramics (UHTCs). A large number of studies have been devoted to a search for additives to the diborides acting as sintering activators and corrosion inhibitors. In studies of diboride based UHTCs, recent research has demonstrated that mechanical properties and high-temperature oxidation/ablation resistance are enhanced with the addition of silicon carbide (SiC) over a wide range of SiC content.[1–5] The addition of some nitrides (Si_3N_4, AlN, ZrN), silicides ($MoSi_2$, $ZrSi_2$) and carbides (B_4C, WC) in small quantities (up to 5%) have also been shown to enhance sintering of ZrB_2–SiC composites.[6–12] The research until now was focused on assessing the impact of silicide additives on the rate of high-temperature oxidation of ZrB_2–SiC ceramics. It was shown that additions of silicides ($ZrSi_2$, $MoSi_2$, $TaSi_2$, etc.) improve the oxidation resistance of ZrB_2–SiC ceramics.[13–19] The effect of additives of silicides on the mechanical properties of ceramics was investigated to a lesser extent.

A wide combination of technical requirements is imposed on high performance structural ceramics materials. Sufficiently low creep rate, as well as high resistance to high-temperature oxidation and corrosion, and a high level of strength and fracture toughness are among the most important ones. This complex set of material property requirements, in turn, leads to a combination of contradictory and often incompatible demands to the structural state and composition of ceramics. Therefore, development of structural ceramics always involves optimization of the structural state and composition on the basis of some compromise in properties.

In this paper, the dependence of basic mechanical properties on composition and structure characteristics of ZrB_2–SiC($ZrSi_2$) ceramics was investigated. A number of experiments on sintering in this system, with variations in the ZrB_2–$ZrSi_2$ and ZrB_2–SiC ratios have been carried out in order to optimize the composition.

The peculiarities of raw materials, conditions of charge preparation and hot pressing as well as structure, phase formation and resistance of ceramics to high-temperature oxidation are discussed in another paper in this volume.[20]

2. Materials and methods

The α-SiC powder used in the study was UF10 grade produced by the H.C. Starck Company, Germany. The ZrB_2 and $ZrSi_2$ powders were synthesized at the Institute for Problems in Materials Science of National Academy of Science (Ukraine) using carbon-thermal reduction reactions of the appropriate oxides. The obtained powders were characterized using

* Corresponding author. Tel.: +380 444241321; fax: +380 444243502.
E-mail addresses: oleggrig@ipms.kiev.ua (O.N. Grigoriev), ism@voliacable.com, ism@ipms.kiev.ua (S.M. Ivanov).

0955-2219/$ – see front matter © 2010 Published by Elsevier Ltd.
doi:10.1016/j.jeurceramsoc.2010.03.022

XRD and chemical analyses. Typical ZrB_2 powder contained 78.8 wt.% B and <0.1 wt.% O. The powder batches contained up to 0.7 wt.% C which corresponded to 3.5% B_4C. $ZrSi_2$ powder with particles size $D_{50} = 30$ μm had the following chemical composition: 61.0 wt.% Zr, 37.0 wt.% Si, and <0.1 wt.% Fe.

Grinding of powders was carried out using an acetone medium and ZrB_2 grinding balls. Grinding balls were made of pure powders by hot pressing. The lining of the mill was fabricated out of a caprolactone wear-resistant polymer. Grinding was carried out to obtain a starting average particle size of ~3 μm. Optimum particles dispersions were achieved by planetary milling, providing sufficiently small grain sizes for hot pressing (from 1.1 to 2.5 μm), as determined by a laser particle size analyzer (Laser Micron Sizer, Japan).

Hot pressing was conducted using an induction heating unit in graphite dies. The temperature of isothermal sintering under load was in the range of 1800–2150 °C, pressure 26–30 MPa, time of isothermal densification 10–40 min, heating rates up to 100 °C/min. Sintering studies were performed in order to obtain ceramics with an average grain size of about 15–20 μm to minimize creep at high temperatures.

Bending strength of the samples (4–12 specimens per data point) was measured by both three and four-point bending using spans of 30 mm and 20 mm × 40 mm. For high-temperature measurements of strength in air in three- and four-point bending, a special fixture was fabricated from hot-pressed silicon nitride. The maximum testing temperature was 1400 °C.

The Vickers hardness was measured at loads in the range of 2–300 N. Hardness of brittle materials measured with a sharp indenter under small loads is a characteristic of material resistance to elastic–plastic deformation. With higher loads the role of fracture is increasing and hardness decreases. Hardness number in this case characterizes resistance of material to elastic deformation, brittle fracture and compaction of fractured material. For the certification of obtained ceramics we used indentation methods to determine not only hardness but also strength characteristics as well as fracture toughness. A new model of indentation of brittle heterophase materials was developed,[21] in which macrohardness is considered as a characteristic of resistance of materials to fracture and, consequently, it depends on both strengths under uniaxial compression (Y) and tension (σ_f), as well as on the so-called microstructural strength[22] ($S = Y\sigma_f/(Y - \sigma_f)$). The indentation fracture toughness was determined according to ref. [23]. Method[23] uses the Lawn relation[24] $K_{IC} = \beta(P/C^{3/2})$, where β is determined analytically. Values of K_{IC}, determined by this method are similar in magnitude to the values obtained by the SEVNB (single-edge V-notched beam) method, although less than that determined by other methods, e.g., IF (indentation fracture) method.[25]

3. Results and discussion

3.1. UHTC structure and composition optimization

The region of brittle fracture of ceramics under study extends up to 1600–2000 °C. At higher temperatures (2000–3200 °C), mechanical behaviour is determined by plastic deformation that can also lead to fracture. The peculiarity of ceramic materials, where relaxation of internal stresses is absent in the first interval and stress relaxation is impeded in the second, is determined by the extreme importance of stress concentrators and non-homogeneities. This is the reason why the analysis of the stress–strain state of the ceramic composite is so important for investigation of dependence of fracture characteristics on non-homogeneous fields of internal stresses.

Table 1
Some properties of zirconium diboride and silicon carbide[27].

Phases	E (GPa)	Poisson's ratio, ν	α ($\times 10^{-6}$/K)	K_{IC} (MPa m$^{1/2}$)
ZrB_2	495	0.121	6.2	4
SiC	460	0.17	4.5	3

The present analysis considers thermal residual stresses, stipulated by the difference in linear expansion coefficients (α) of composite phases. Taking into account the material's macroscopic homogeneity and isotropic distribution of phase components, one can make an assumption as to the hydrostatic nature of the tensile and compressive stresses in each of its phase $(\sigma_{11})_i = (\sigma_{22})_i = (\sigma_{33})_i = \bar{\sigma}_i$, governed by the conditions of stress equilibrium $\sum Y_i\bar{\sigma}_i = 0$. Calculation of internal thermal stresses in composites was performed on the basis of a statistical approach,[26] using physical characteristics for each phase (see Table 1) and the following relations:

$$\langle\sigma_{ij}\rangle_1 = Y_2\eta\delta_{ij}, \quad \langle\sigma_{ij}\rangle_2 = -Y_1\eta\delta_{ij}, \quad \eta = \frac{\gamma}{K_1K_2 + \langle K\rangle\gamma} \times \{(K_1 - K_2)p_s - 3K_1K_2[(\alpha_1 - \alpha_2)\,\Delta T + (l_1 - l_2)]\},$$

$$\gamma = \left(\frac{4}{3}\right)\langle G\rangle, \quad \langle G\rangle = Y_1G_1 + Y_2G_2,$$

$$\langle K\rangle = Y_1K_1 + Y_2K_2$$

The intensity of internal stresses could be characterized by internal energy, which relates to the unit of microvolume

$$\langle U\rangle = Y_1\langle U_1\rangle + Y_2\langle U_2\rangle$$

The internal energies of components are defined as:

$$\langle U_1\rangle = \frac{\eta^2Y_2^2}{2K_1}, \qquad \langle U_2\rangle = \frac{\eta^2Y_1^2}{2K_2},$$

where G_i is the shear modulus of ith phase, E is the Young's modulus; ν is the Poisson's ratio, Y_i is the volume fraction of ith phase, α_i are the coefficients of linear temperature expansion, K_i is the modulus of bulk compression of ith phase, l_i is the specific volume of ith component, p_s is the external pressure at sintering, and U_i is the internal energy of elastic strain of ith phase.

At known values of elastic and thermal characteristics of composite phases, the value of internal stresses is determined by the ΔT – temperature difference between the temperature of the viscous–elastic transition T_{ve} and the final temperature, down to which the material is cooled after hot pressing (typically, room temperature).

From the results of calculations (Fig. 1), the internal stresses are tensile in ZrB_2 and compressive in SiC. With an increase of

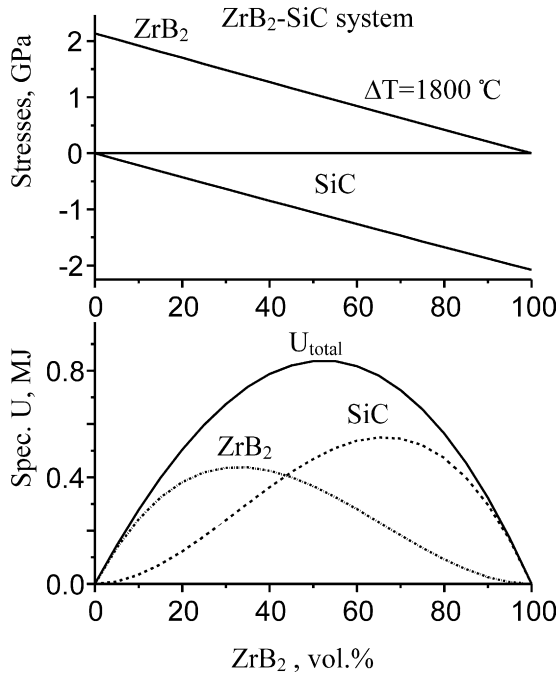

Fig. 1. The dependencies of internal stresses and specific energy of elastic strains U in SiC and ZrB_2 composite phases versus ZrB_2 content.

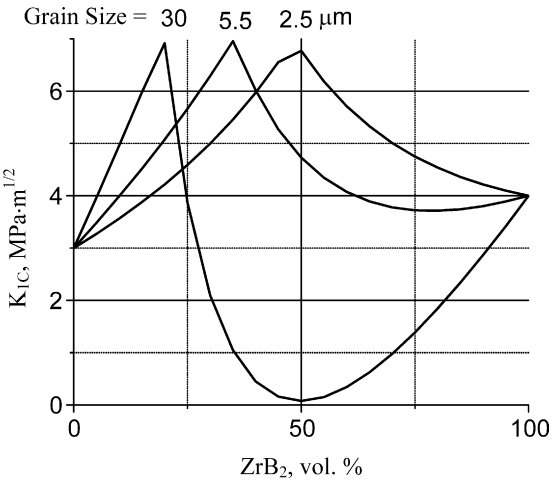

Fig. 2. Influence of grain size and composition on the fracture toughness of ZrB_2–SiC ceramics.

any phase content, stress level in it decreases. The dependencies of specific energy of elastic deformation on composition are presented in Fig. 1. The values of specific energies of elastic deformation of the phases are maximized in the range of 25–40% of the same phase content. Thus, the total specific energy of elastic deformation of the composite (U_{total}) was found to have a maximum at the equivolume phase content. This determines the tendency of the ceramics to spontaneously fracture due to thermal residual stresses.

An increase of composite fracture toughness and strength can thus be achieved by appropriate selection of components, such as the ratios of their volume fractions and grain sizes, when the matrix, subjected to the effect of residual thermal stresses, will be in a compressed state, and the isolated second phase inclusions are in a tensile state. The crack would than be forced to propagate in a compressed matrix, coming around the second phase due to the peculiarities of a non-homogeneous stress field.

In this study, a mathematical formulation for the fracture toughness criteria in a ceramic matrix composite, and an optimization method for composite structure and composition,[28] was used to take into account the fields of internal thermal stresses.

In simple cases, composite fracture toughness is expressed by the relation:

$$\tilde{K}_{\text{I}} = \tilde{K}_{\text{IC}} = \min_i(a_i^{-1}(K_{\text{IC}}^i - D\sigma^{ri})),$$

and optimum composition is determined by the criteria:

$$\tilde{K}_{\text{IC}}^{\text{opt}} = \underset{Y}{\text{MAX}}\underset{i}{\text{MIN}}(a_i^{-1}(K_{\text{IC}}^i - D\sigma^{ri})),$$

$$\alpha_i = \frac{G_i|Y_i|}{\sum_{i=1}^{N} G_i|Y_i|} \le 1, \qquad D = \frac{2\sqrt{C}}{\pi},$$

where σ^{ri} is the residual thermal stresses, G_i is the shear modulus of ith phase, C is the typical size of initial defects (cracks), K_{I} is the stress intensity factor for normal fracture (opening mode), and K_{IC}^i is the fracture toughness of ith component of composite.

Composite parameters used in calculation of K_{IC}, are elastic phase characteristics, fracture toughness values of composite components and parameter D.

Generally, introduction of a high-TEC (thermal expansion coefficient) component into a composite increases fracture toughness. The maximum of fracture toughness with increase of mismatch of TEC, elastic characteristics as well as typical size of structural defects (microcracks) shifts to lower second phase contents.

Results of the calculations are presented in Fig. 2. According to the calculations, the compositions based on silicon carbide matrix appear to be the preferable ones. For the purpose of these calculations, the size of the microcracks was assumed to be equal to the average grain size, the latter considering the same for both phases of the composite. In the ZrB_2–SiC system, differences in elastic characteristics and coefficients of thermal expansion are moderate. The calculations show that high fracture toughness can be achieved in a range of high zirconium diboride content (45–50 vol.%) with a small grain size (~2 μm). With an increase in grain size, the fracture toughness maximum shifts in the direction of lower zirconium diboride content while the minimum of fracture toughness forms in the range of equivolume content of components. For example, at defect sizes of approximately 30 μm (this size can match the size of grains or agglomerates of ZrB_2) fracture toughness in the range of 45–50 vol.% ZrB_2 decreases to values near zero. This corresponds to the criterion of spontaneous fracture of ceramics under the action of thermal

Table 2
The composition of some ZrB_2–$ZrSi_2$–SiC ceramics and regimes for their hot pressing.

Samples	Charge composition (vol.%)			Bending strength/standard deviation[a] (MPa)	Porosity (%)
	SiC	ZrB_2	$ZrSi_2$		
US1	0	100	0	325/35	10
US2	17	83	0	460/46	0
US20	18.6	81.4	0	499/52	0
US3	23	77	0	465/54	0
US4	50	50	0	365/42	6
US6	65	35	0	270/31	14
USS1	0	93.5	6.5	370/32	11
USS22	17.6	78	4.2	479/35	0
USS23	17.2	75.4	7.4	403/31	0
USS3	26	67	7	478/70	1
USS4	49	47	4	436/40	0
USS41	49	49	2	460/17	0
USS42	49	47.4	3.6	400/30	0
USS43	49	43.9	7.1	420/44	3
USS44	49	41.3	9.7	451/30	3
USS45	49	38.8	12.2	340/37	6
USS46	49	37.2	13.8	354/35	6
USS6	60	37	3	380/40	6

[a] Bending strength of the samples was measured in four-point bending using 30 mm base.

residual stresses.

$$2C_{cr} = 2\underset{i}{\mathrm{MIN}}\left[\left(\frac{\alpha_i^{-1}K_{\mathrm{IC}}^{i}}{(2/\sqrt{\pi})\sigma^{ri}}\right)^2\right],$$

where C_{cr} is the critical grain size for spontaneous failure under the effect of thermal stresses.

It is well known that reduction of grain size is accompanied by a strength increases at ambient temperature. At present, there are technological sintering processes which indeed allow manufacture of ZrB_2–SiC ceramics with an average grain size of 2 μm or less. In the region of equivolume phase contents thermo-mechanical model predicts a maximum in both fracture toughness and strength values due to both peculiarities of the internal stress–strain state and fine grain structure ($d_{gs} \sim 1$–2 μm). However, at high temperatures fine grain size is expected to increase both creep and high-temperature oxidation rate.[29,30] Powders used for this study were selected to provide a grain size of about 10–15 μm, which ensured a basic level of properties over a wide temperature range. In order to preserve the necessary level of low-temperature fracture toughness at such grain size (compensating for a certain decrease of strength because of structural roughening), ZrB_2 content should be reduced to 25–30%, i.e. composites became SiC-based instead of being ZrB_2-based.

3.2. Mechanical properties at room temperature

3.2.1. The influence of $ZrSi_2$ additives on sinterability and strength characteristics

Compositions of ZrB_2–SiC and ZrB_2–$ZrSi_2$–SiC ceramics for identical regimes of fabrication (temperature of isothermal sintering under load was 2150 ± 25 °C, pressure 30 MPa, time of isothermal densification 10–15 min) are given in Table 2. The values of bending strength and sample porosity are also presented in the table. Samples of the US series did not contain $ZrSi_2$ additives; in samples USS1–USS6 the content of silicon carbide was varied at a fixed ZrB_2:$ZrSi_2$ ratio (92:8). Samples of the USS series had a fixed content of silicon carbide (49 vol.%) and a variable ratio of ZrB_2:$ZrSi_2$.

The introduction of zirconium silicide, all other factors being the same, widens the range of silicon carbide concentrations where formation of pore-free materials can be obtained. For ZrB_2–SiC ceramics, non-porous samples were achieved at SiC contents of about 20 vol.%. For the ZrB_2–$ZrSi_2$–SiC system, non-porous ceramics were obtained in the range of SiC contents from 20 to 50 vol.% (Table 2). Analysis of ceramics of the USS41–USS46 set shows that small amounts of $ZrSi_2$ additives (2–4%) are sufficient for sintering activation. Further increases of $ZrSi_2$ content, up to 14%, was accompanied by an increase of porosity due to interaction of $ZrSi_2$ with components of the ceramics. Bending strengths of ZrB_2–SiC and ZrB_2–$ZrSi_2$–SiC systems had similar values (Table 2).

It was found that the hardness of zirconium boride (US1-sample) with a porosity level up to 10% falls from 16.5 to 9 GPa with increasing indentation load from 2 to 300 N (Fig. 3a). These results are consistent with well-known data[31] for ZrB_2 (HV1.0 = 8.7 GPa) and ZrB_2 + 5% Si_3N_4 (HV1.0 = 13 GPa).

At the same time, the introduction of zirconium disilicide into zirconium diboride in the amount of 6.5% (USS1-sample) led to a significant decrease in the hardness of zirconium diboride to the range of 6.5–12 GPa corresponding to indentation loads in the range of 2–300 N (Fig. 3b). Hardness decrease was associated with the interaction of zirconium boride and silicide during sintering with the formation of a new phase ZrBC of variable composition and other intermediate compounds (see paper[20] in this issue).

Studies of the mechanical behaviour of ZrB_2–SiC–$ZrSi_2$ ceramics, under fixed SiC content, were carried out on the USS41–46 compositions. The results of hardness measurements

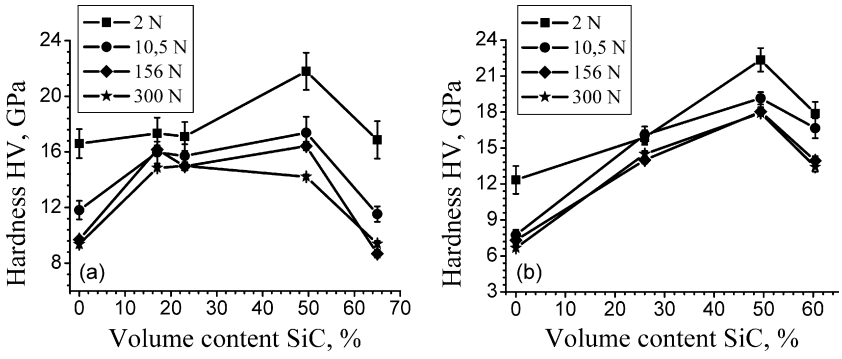

Fig. 3. Hardness of ceramics versus SiC content: (a) ZrB_2–SiC (US1, . . ., US6 samples) and (b) ZrB_2–$ZrSi_2$–SiC (USS1–USS3–USS4–USS6 samples with ZrB_2:SiC ratio equal to 92:8).

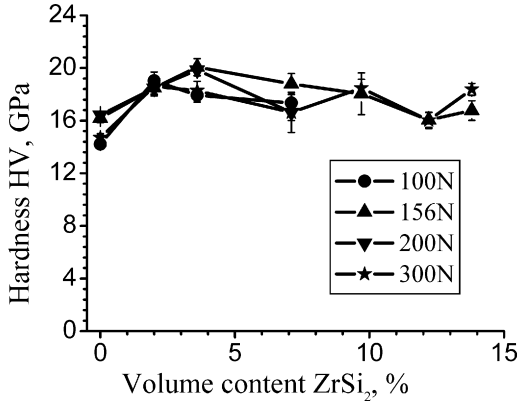

Fig. 4. Hardness of (ZrB_2–$ZrSi_2$)–49 vol.% SiC ceramics (US4, USS41–USS46 samples) versus $ZrSi_2$ content at different indentation loads.

(Fig. 4) of these materials showed that high hardness values (16–20 GPa) were preserved over a wide range of indentation loads (100–300 N). Decreasing the indentation load to 2 N resulted in an increase in hardness up to 18–25 GPa for all samples. At even higher indentation loads the hardness changed only slightly with little variance at the highest load. Composites containing 2–10 vol.% $ZrSi_2$ were characterized by maximum hardness. The data obtained are higher than those of ceramics ZrB_2–SiC (USS4, see Fig. 4), as well as higher or comparable with published data (HV1.0 = 14.2–14.6 GPa for ZrB_2–SiC ceramics with Si_3N_4-additives[31]; HV10 = 15.2–16.7 GPa and HV10 = 19.9–21.3 GPa for ZrB_2–SiC ceramics with SiC grain sizes 0.8–1.8 μm and 80 nm respectively[32]; HV1.0 = 17.7–18.2 GPa for Zr(Hf)B_2–SiC ceramics[33] and HV0.2 = 17.5–20.7 GPa for ZrB_2–SiC ceramics with different starting SiC particles sizes (SiC–UF05, UF10 and UF25 powders[34]).

Using hardness measurements and length measurements for radial cracks formed near a hardness indent, Weibull statistical distributions for the contact strength[21,35] of ZrB_2–SiC and ZrB_2–$ZrSi_2$–SiC composites were built (Fig. 5a). In the majority of cases the distributions proved to be bimodal, i.e. they contained two straight line regions corresponding to two differing crack populations — "long" and "short" cracks. The nature of long versus short crack formation has been discussed previously in the literature.[35] The Weibull modulus for "long" cracks of ZrB_2–SiC ceramics varied in the range of 9–16. Statistical distributions for the contact strength of ZrB_2–SiC–$ZrSi_2$ ceramics are presented in Fig. 5b. The Weibull modulus *m* determined for the cracks varied in the range of 17–24. Higher values of Weibull modulus of ZrB_2–SiC–$ZrSi_2$ ceramics point to its higher structural homogeneity in comparison with ZrB_2–SiC ceramics.

With increasing load the length of the "long" cracks was found to increase (Fig. 5a). The displacement of the Weibull distributions to the left is direct evidence for decreasing contact strength. A separate analysis of the population of "long" cracks showed that with increasing load contact strength decreases sharply and reaches approximately constant value in the 200–300 N load range (Figs. 6 and 7). This decrease in contact strength with increasing load is due to a scale effect

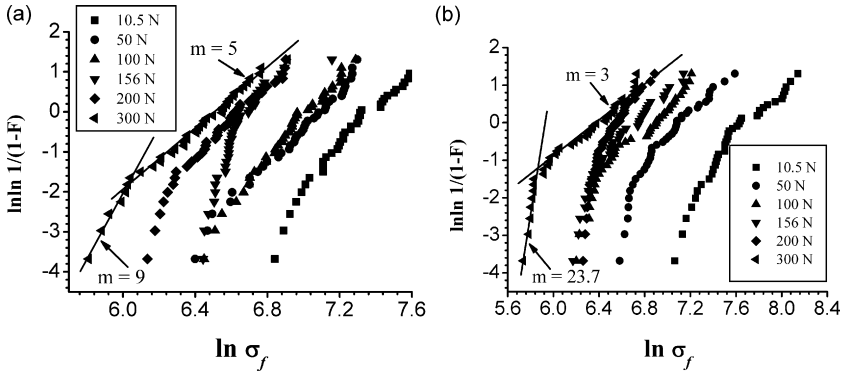

Fig. 5. Weibull statistical distributions for contact strength: (a) ZrB_2–65 vol.% SiC (US4) and (b) ZrB_2–4 vol.% $ZrSi_2$–49 vol.% SiC (USS4) composites.

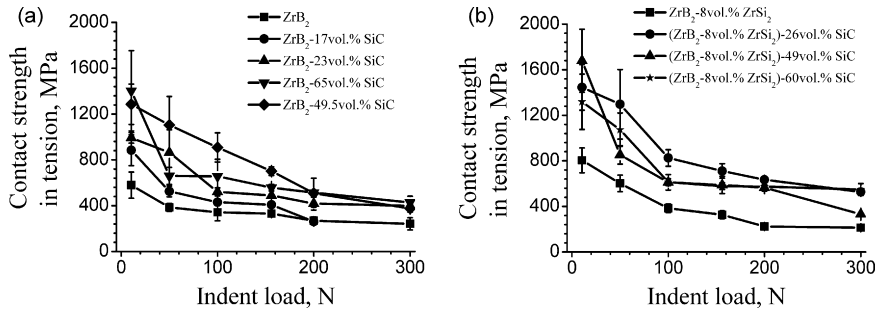

Fig. 6. Contact strength in tension of ceramics versus indentation load: (a) ZrB_2–SiC (US1–US6 samples) and (b) ZrB_2–$ZrSi_2$–SiC (USS1–USS6 samples); error bars, standard deviation.

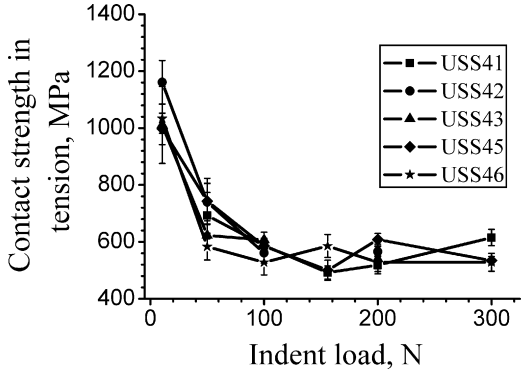

Fig. 7. Contact strength in tension of (ZrB_2–$ZrSi_2$)–49 vol.% SiC ceramics versus indentation load.

(dependence of the strength on the sample size or the volume of fractured material), as is usual for contact measurements.

As in the case of hardness, zirconium diboride has a minimum contact strength throughout the range of indenter loads (Fig. 6). Contact strength of zirconium diboride (240 MPa at indenter load 300 N) decreases to 215 MPa in the samples with additions of zirconium silicide. Consequently, zirconium silicide additives reduce contact strength and hardness of zirconium diboride. However, in ZrB_2–SiC ceramics the opposite phenomenon is observed — zirconium silicide additives help to increase contact strength from 400 to 550–600 MPa at high indentation loads (300 N) (Figs. 6 and 7). The difference in the behaviour of ZrB_2–$ZrSi_2$ and ZrB_2–$ZrSi_2$–SiC ceramics are attributed to differences in phase composition of these materials — the presence of a large quantity of ZrBC phase in the first ceramics according to the X-ray phase analysis, but only a small amount of this phase (up to 3 vol.%) and additional grain-boundary amorphous phase in the second ceramics.[20]

3.2.2. *The influence of SiC content on mechanical properties*

Hardness in the range of loads of 10–300 N in nearly pore-free ZrB_2–20% SiC ceramics is high enough and is equal to 15–16 GPa (Fig. 3a). In accordance with discussion in Section 3.1 and Fig. 2, there is a maximum in hardness with increasing content of silicon carbide up to about 60–70 vol.%. But with the increase in SiC content the porosity level also increases, and at about 50 vol.% SiC the porosity level of material is more than 5%. Nevertheless, at this porosity level the composite hardness is sufficiently high (16–18 GPa) and even exceeds that of the pore-free material. For the ZrB_2–$ZrSi_2$–SiC system, within the 20–50% range of SiC concentrations, porosity is approximately constant (less than 1%) and the hardness achieves a maximum at high SiC contents (Fig. 3b). Thus, the increase of hardness up to 18–19 GPa (for loads in the range of 10–300 N) at 20–50 vol.% SiC reflects the influence of silicon carbide only on the composite properties. Further increases in SiC content, up to 60–65 vol.%, is accompanied by a decrease in hardness to 8.5–11.5 and 14–17 GPa in ZrB_2–SiC and ZrB_2–$ZrSi_2$–SiC ceramics, respectively (Fig. 3).

The results of the fracture toughness measurements on ZrB_2–SiC and ZrB_2–$ZrSi_2$–SiC composites are presented in Fig. 4. The increase in SiC volume content in both ZrB_2–SiC and ZrB_2–$ZrSi_2$–SiC composites (Fig. 8) resulted in an increase in fracture toughness (2–3.4 MPa $m^{1/2}$). Such behaviour in the

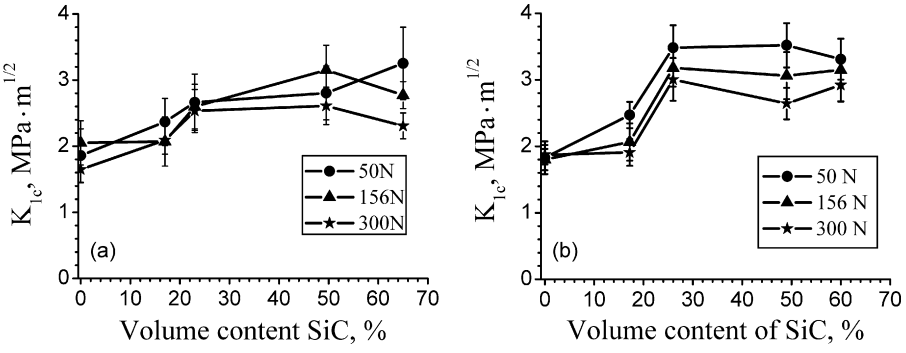

Fig. 8. Fracture toughness of ceramics versus SiC content: (a) ZrB_2–SiC (US1, . . ., US6 samples) and (b) ZrB_2–$ZrSi_2$–SiC (USS1–USS3–USS4–USS6 samples with ZrB_2:$ZrSi_2$ ratio equal 92:8).

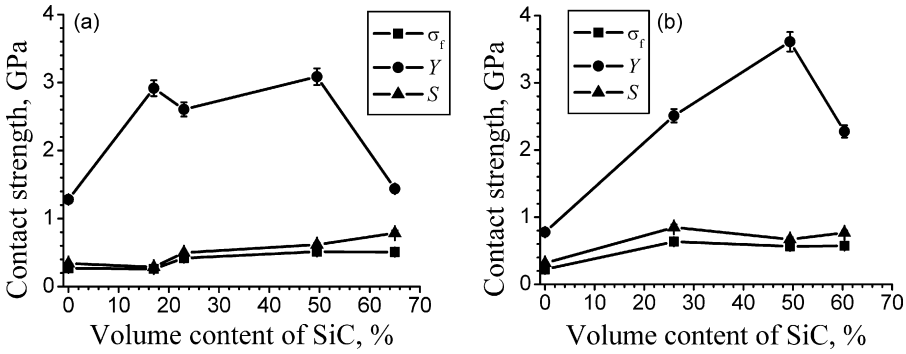

Fig. 9. Contact strength in tension (σ_f) and compression (Y) as well as microstructure strength (S) of ceramics versus SiC content (load 200 N): (a) ZrB_2–SiC (US1–US6 samples) and (b) (ZrB_2–8 vol.% $ZrSi_2$)–SiC (USS1–USS6 samples).

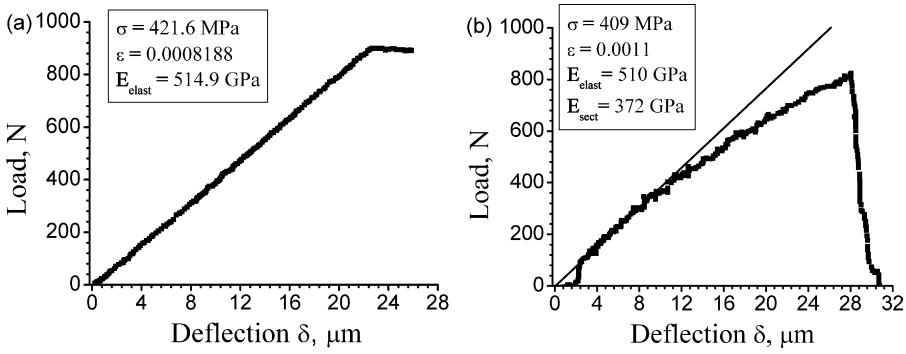

Fig. 10. Stress–strain curves (four-point bending, spans of 20 mm × 40 mm) for the US20 samples at RT (a) and 1400 °C (b).

ZrB_2–$ZrSi_2$–SiC composites is caused by both stress redistribution between the phases and effects of mesoscopic mechanisms of toughness (cracks tilting near inclusions of secondary phases).[1,5] However, increasing $ZrSi_2$ content did not markedly affect fracture toughness, with toughness remaining in the range of 2–3.4 MPa $m^{1/2}$.

The results of the calculations of contact strength in tension (σ_f) and compression (Y), as well as the measured microstructural strength of ZrB_2–SiC and ZrB_2–$ZrSi_2$–SiC composites, are presented in Fig. 9. Increased values of contact strength in compression for the ZrB_2–SiC system were reached over a wide range of compositions. For the ZrB_2–$ZrSi_2$–SiC composites the maximum in contact strength in compression was observed for high silicon carbide contents. The dependence of Y on the SiC content is similar to dependencies of hardness (Fig. 3) and is in accordance with the results and discussion from Section 3.1. Composites in the ZrB_2–$ZrSi_2$–SiC system, compared to the ZrB_2–SiC composites, exhibited a higher level of contact strength in tension and microstructural strength. Microstructural strength is the strength of ceramics in micro-volumes and it can be interpreted, for example, as grain-boundary strength. Thus, the introduction of SiC in both types of composites increased microstructural strength and decreased the damage of the material under the application of thermal and mechanical loads.

As a whole, the dependencies of the mechanical properties on silicon carbide content, for both the ZrB_2–SiC and ZrB_2–$ZrSi_2$–SiC systems, are in good agreement with the conclusions from the thermo-mechanical model (see Section 3.1). Consequently, the field of interfacial thermal residual stresses determines the mechanical behaviour of the studied ceramics, at low temperatures.

3.3. High-temperature strength

Bending strength at temperatures up to 1400 °C were measured and compared to the bending results at room temperature (Fig. 10). A stress–strain curve for one of the compositions in the ZrB_2–SiC system (US20: 81.4 vol.% ZrB_2 + 18.6 vol.% SiC) at room temperature was practically linear (Fig. 10). Young's modulus at room temperature was determined to be 515 GPa (with an accuracy of ~2%), and bending strength was 420 MPa (four-point bending with a base of 40/20 mm). At a temperature of 1400 °C the stress–strain curve for the same composition

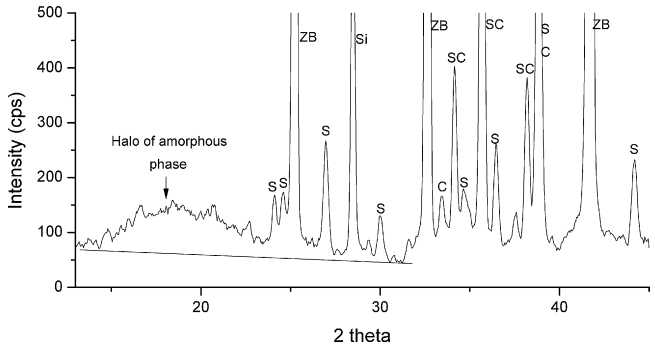

Fig. 11. XRD pattern of USS46 sample with halo of amorphous phase and crystalline phases: ZB (ZrB_2, 34-423); Si (Si-etalon, 27-1402); SC (SiC,6H,3C); C (Zr(BC)); S ($ZrSi_2$, lattice parameters increased on 32-1499).

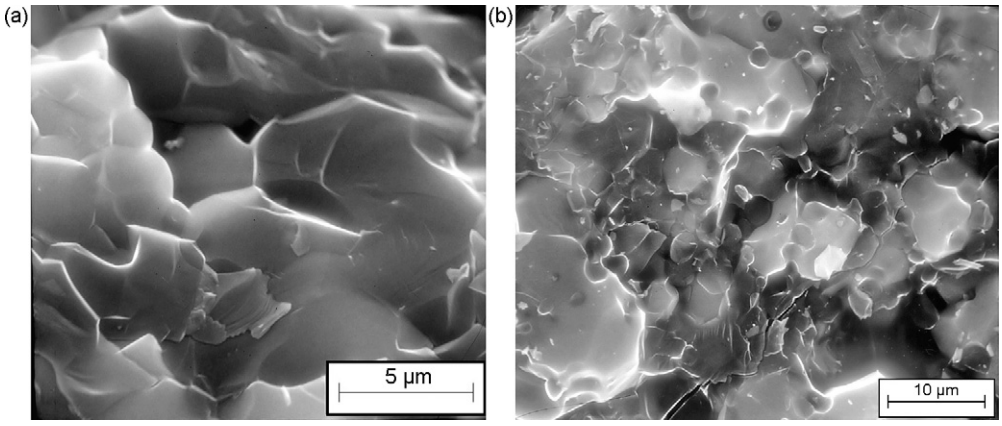

Fig. 12. Fracture surfaces of ceramics: (a) ZrB_2–49 vol.% SiC–2 vol.% $ZrSi_2$ and (b) ZrB_2–49 vol.% SiC–14 vol.% $ZrSi_2$.

exhibits significant nonlinearity. The use of zirconium silicide as an additive for sintering activation and enhancing resistance to high-temperature oxidation[20] is connected with the presence of grain-boundary amorphous layers. Usually, amorphous layers at the grain boundaries are responsible for grain-boundary creep of the composite and nonlinearity in the stress–strain curve at high temperatures, with the creep rate (and rate of growth of microcracks at creep) having a functional dependence on the thickness and viscosity of grain-boundary layers, as well as grain size.[36] The equilibrium phase diagram for the Zr–Si system points out to a peritectic type of $ZrSi_2$ decomposition with the appearance of a liquid Zr–Si phase at hot pressing temperatures exceeding 1620 °C. The interaction of the Zr–Si liquid with the basic phases of the composite leads to the formation of a new phase, based on the ZrC lattice, as well as enrichment of the liquid with boron. The XRD data indicate the essential reduction of lattice parameters of the new phase,[20] compared with zirconium carbide, due to formation of solid solutions in the Zr(C,B) system. The volume content of this new cubic phase does not exceed 3%, which qualitatively corresponds to microscopic observations. The linear dependence between $ZrSi_2$ and Zr(C,B) contents exists only at small $ZrSi_2$ contents. XRD shows that in ceramics with higher $ZrSi_2$ contents (>8–10 vol.%), residual Zr–Si liquid is partially crystallized during cooling as zirconium silicide $ZrSi_2$ with higher lattice parameters (compared to the initial state), and partially remains in an amorphous state (Fig. 11). Thus, at small amounts of silicide additives the liquid phase is almost entirely consumed by the Zr(C,B) phase. However, the higher zirconium silicide contents leads to an excess of Zr–Si–B–(O) liquid phase, which on cooling transforms into residual amorphous phase and modified crystalline zirconium silicide. The presence of these phases even leads to grain-boundary porosity (Fig. 12) which would be expected to influence the mechanical behaviour of these ceramics at high temperature.

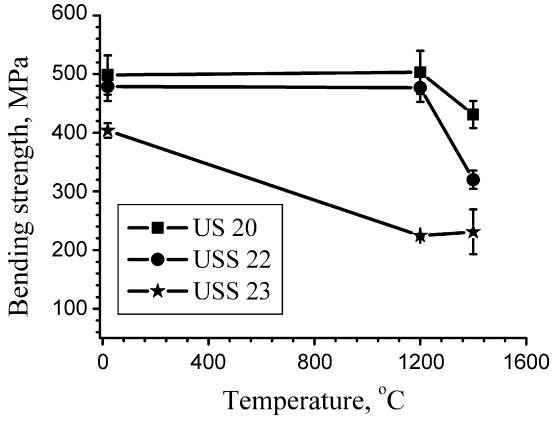

Fig. 13. Temperature dependence of bending strength for ZrB_2–SiC and ZrB_2–$ZrSi_2$–SiC ceramics.

The Young's modulus from the linear portion of the curve is still reasonable (510 GPa). The bending strength of this composition at 1400 °C, compared to that at room temperature, remains almost constant (~410 MPa). Thus, the US20 ceramics, which is regarded as a base material, has satisfactory bending strength and mechanical stability over a wide temperature range.

The temperature dependences of the bending strength for some of the other US and USS compositions are presented in Fig. 13. As can be seen from the data, incorporation of $ZrSi_2$ into the composite led to an essential softening of the ceramics above 1000 °C. The softening of the composites with $ZrSi_2$ additives is connected to a grain-boundary amorphous phase with insufficient viscosity at high temperatures.

The presented results show that the introduction of zirconium disilicide, as a sintering activation addition, is accompanied by an improvement of some mechanical properties at lower temperatures (hardness, contact strength, Weibull modulus), but loss of strength at elevated temperature (1400 °C).

4. Conclusion

The mechanical properties of ZrB_2–SiC and ZrB_2–SiC–$ZrSi_2$ hot-pressed ceramics (with grain sizes 10–15 μm) in the composition range 0–60 and 0–14 vol.% of SiC and $ZrSi_2$, respectively, were studied. The introduction of SiC improves mechanical properties (hardness of 18–20 GPa, fracture toughness of 3.5 MPa $m^{1/2}$, bending strengths of 400–500 MPa, contact strength in tension of 400–650 MPa) at low temperature. Further, the maximum in the strength characteristics is formed at high SiC content. ZrB_2–$ZrSi_2$–SiC ceramics preserved high hardness values over a wide loading

range, and in the range of 100–300 N the hardness did not vary significantly. The dependencies of mechanical properties of the ceramics on silicon carbide content are in good accordance with the conclusions of a thermo-mechanical model for mechanical properties of heterogeneous ceramics.

The introduction of $ZrSi_2$ (all other factors being the same) assists in activating sintering and therefore reduces porosity in ZrB_2–SiC based ceramics and widens the range of silicon carbide concentrations where formation of pore-free materials have been observed. The addition of $ZrSi_2$ (up to 4 vol.%) slightly affects the bending strength of ceramics but essentially improves the contact strength and homogeneity characteristic (Weibull modulus $m = 17$–24) at low temperature. However, at high-temperature (1400 °C) strength decreases to 320 MPa for ceramics with $ZrSi_2$ additions.

Acknowledgement

This work was carried out under Science and Technology Centre of Ukraine Project P286.

References

1. Grigoriev ON, Gogotsi YuG, Subbotin VI. Structure and properties of SiC–MeB_2 ceramics. *Mater Res Soc Symp Proc* 1998;**481**:249–54.
2. Opeka MM, Talmy IG, Wuchina EJ, Zaykoski JA, Causey SJ. Mechanical, thermal and oxidation properties of refractory hafnium and zirconium compounds. *J Eur Ceram Soc* 1999;**19**:2405–14.
3. Monteverde F, Scatteia L. Resistance to thermal shock and to oxidation of metal diborides—SiC ceramics for aerospace application. *J Am Ceram Soc* 2007;**90**(4):1130–8.
4. Monteverde F. Beneficial effects of an ultra-fine α-SiC incorporation on the sinterability and mechanical properties of ZrB_2. *Appl Phys* 2006;**A82**:329–37.
5. Grigoriev ON, Gogotsi YuG, Brodnikovsky NP, Subbotin VI. Development and properties of SiC–B_4C–MeB_2 ceramics. *Powder Metall* 2000;**5/6**:29–42 [Transl. from Russian].
6. Monteverde F. The thermal stability in air of hot-pressed diboride matrix composites for uses at ultra-high temperatures. *Corros Sci* 2005;**47**:2020–33.
7. Gach M, Ellerby D, Irby E, Beckman S, Gusman M, Jonson M. Processing, properties and arc jet oxidation of hafnium diboride/silicon carbide ultra high temperature ceramics. *J Mater Sci* 2004;**39**:5925–37.
8. Monteverde F, Bellosi A. Effect of the addition of silicon nitride on sintering behavior and microstructure of zirconium diboride. *Scripta Mater* 2002;**46**:223–8.
9. Fahrenholtz WG, Hilmas GE, Talmy IG, Zaykoski JA. Refractory diborides of zirconium and hafnium. *J Am Ceram Soc* 2007;**90**(5):1347–64.
10. Chamberlain AL, Fahrenholtz WG, Hilmas GE, Ellerby DE. High-strength zirconium diboride-based ceramics. *J Am Ceram Soc* 2004;**87**(6):1170–2.
11. Silvestroni L, Sciti D. Effects of $MoSi_2$ additions on the properties of Hf– and Zr–B_2 composites produced by pressureless sintering. *Scripta Mater* 2007;**57**:165–8.
12. Lavrenko VA, Dayatel VD, Lugovaya ES. Interaction of materials ZrB_2–$ZrSi_2$ system with oxygen at high temperature. *Powder Metall* 1982;**6**:56–8 [Transl. from Russian].
13. Talmy IG, Zaykovski JA, Opeka MM. High-temperature chemistry and oxidation of ZrB_2 ceramics containing SiC, Si_3N_4, Ta_5Si_3, and $TaSi_2$. *J Am Ceram Soc* 2008;**91**(7):2250–7.
14. Peng F, Speyer RF. Oxidation resistance of fully dense ZrB_2 with SiC, TaB_2, and $TaSi_2$ additives. *J Am Ceram Soc* 2008;**91**(5):1489–94.
15. Talmy IG, Zaykovski JA, Opeka MM, Smith AH. Properties of ceramics in the system ZrB_2–Ta_5Si_3. *J Mater Res* 2006;**21**(10):2593–9.
16. Guo SQ, Nishimura T, Mizuguchi T, Kagawa Y. Mechanical properties of hot pressed ZrB_2–$MoSi_2$–SiC composites. *J Eur Ceram Soc* 2008;**28**(9):1891–8.
17. Guo SQ, Kagawa Y, Nishimura T, Tanaka Y. Pressureless sintering and physical properties of ZrB_2-based composites with $ZrSi_2$. *J Eur Ceram Soc* 2009;**29**(4):787–94.
18. Opila E, Levine S, Lorincz J. Oxidation of ZrB_2- and HfB_2-based ultra-high temperature ceramics: effect of Ta additions. *J Mater Sci* 2004;**39**:5969–77.
19. Talmy IG, Zaykovski JA, Opeka MM, Dallek S. Oxidation of ZrB_2 ceramics modified with SiC and group IV–VI transition metal borides. In: McNallan M, Opila E, editors. *High temperature corrosion and material chemistry*, vol. III. Pennington, NJ: The Electrochemical Society, Inc.; 2001. p. 144.
20. Grigoriev ON, Galanov BA, Lavrenko VA, Panasyuk AD, Ivanov SM, Koroteev AV, et al. Oxidation of ZrB_2–SiC–$ZrSi_2$ ceramics in oxygen. *J Eur Ceram Soc* 2010;**30**:2397–405.
21. Galanov BA, Grigoriev ON. Analytic indentation model of brittle solids. In: *Electron microscopy and strength of materials.* Kiev: IPMS Publ.; 2006. p. 4–42 [in Russian].
22. Bogachyov IN, Weinstein AA, Volkov SD. *Introduction in statistical metallurgical science*. Moscow: Metallurgy; 1972, 216 p. [in Russian].
23. Grigoriev ON, Galanov BA, Kotenko VA, Ivanov SM, Kovalchuk VV, Lazhevsky VA. Contact strength and crack growth resistance of brittle materials. *Metallofizika i Noveishie Tekhnologii* 2005;**8**:1001–18 [in Russian].
24. Lawn BR, Wilshaw TR. *Fracture of brittle solids*. New York: Cambridge University Press; 1975, 204 pp.
25. Niihara K, Morena R, Hasselman DPH. Evaluation of K_{IC} of brittle solids by the indentation method with low crack-to-indent ratios. *J Mater Sci Lett* 1982;**1**(1):13–6.
26. Grigoriev ON, Trefilov VI, Khoroshun LP. Residual stresses in two-phase ceramic composites. In: *Proceedings of III All-Union Conf. "Technological Residual Stresses"*. 1988. p. 129–33 [in Russian].
27. Andrievsky AR, Spivac II. *Strength of refractory compounds and materials on its base*. Moscow: Metallurgy; 1989, 368 pp. [in Russian].
28. Galanov BA, Grigoriev ON. Fracture criterion of composites with a ceramic matrix. *Problemy Prochnosti* 1993;**10**:30–40 [Transl. from Russian].
29. Lanin AG, Fedik II. *Thermal stress resistance of materials*. Podolsk: Scientific Institute of Association "LUCH"; 2005, 312 pp. [in Russian].
30. Gogotsi YuG, Lavrenko VA. *Corrosion of high-performance ceramics*. Berlin: Springer-Verlag; 1992, 180 pp.
31. Monteverde F, Guicciardi S, Bellosi A. Advances in microstructure and mechanical properties of zirconium diboride based ceramics. *Mater Sci Eng* 2003;**A346**:310–9.
32. Hwang SS, Vasiliev AV, Padture NP. Improved processing and oxidation-resistance of ZrB_2 ultra-high temperature ceramics containing SiC nanodispersoids. *Mater Sci Eng* 2007;**A464**:216–24.
33. Monteverde F, Bellosi A, Scatteia L. Processing and properties of ultra-high temperature ceramics for space applications. *Mater Sci Eng A* 2007;**485**(1-2):415–21.
34. Zhu S, Fahrenholtz WG, Hilmas GE. Influence of silicon carbide particle size on the microstructure and mechanical properties of zirconium diboride–silicon carbide ceramics. *J Eur Ceram Soc* 2007;**27**:2077–83.
35. Grigoriev ON, Galanov BA, Trunova EG. Statistical characteristics of ceramics contact strength. In: *Electron microscopy and strength of materials.* Kiev: IPMS Publ.; 2001. p. 125–35 [in Russian].
36. Trefilov VI, Grigoriev ON, Trunov GV, Gogotsi GA, Kislyi PS. Development of high-temperatures ceramics for applications in gas turbine engine components. In: Roode M, Ferber MR, Richerson DW, editors. *Ceramic gas turbine components development and characterization*. NY: ASME Press; 2003. p. 397–423.